[1]C. L. Pekeris, H. Lifson, and B. Schiff, Phys. Rev. 137, A137 (1965); 140, A1104 (1965); also, L. C. Green, E. K. Kolchin, and N. C. Johnson, *ibid.* 139, A373 (1965).
[2]I. Waller, Z. Physik 38, 689 (1926).
[3]H. Pfennig and E. Trefftz, Z. Naturforsch. 21a, 697 (1966); C. Deutsch, H. W. Drawin, L. Herman, and Nguyen-Hoe, J. Quant. Spectry. Radiat. Trans. 8, 1027 (1968); C. Deutsch, Mem. Soc. Roy. Sci. Liège 17, 83 (1969).
[4]C. Deutsch, L. Herman, and H. W. Drawin, Phys. Rev. 178, 261 (1969); 186, 204 (1969).
[5]J. O. Hirschfelder, W. Byers-Brown, and S. T. Epstein, in *Advances in Quantum Chemistry*, edited by P.-O. Löwdin (Academic, New York, 1964), Vol. I, p. 315.
[6]A. Dalgarno and N. Lynn, Proc. Phys. Soc. (London) A70, 223 (1957).
[7]W. C. Martin, J. Res. Natl. Bur. Std. 64A, 19 (1960).
[8]A. Dalgarno and J. T. Lewis, Proc. Phys. Soc. (London) A69, 57 (1955); A233, 70 (1956).
[9]L. Pauling and E. B. Wilson, *Introduction to Quantum Mechanics* (McGraw-Hill, New York, 1935), p. 144.
[10]M. J. Seaton, Proc. Phys. Soc. (London) A87, 337 (1966).
[11]J. H. Van Vleck, Proc. Roy. Soc. (London) A143, 679 (1934).
[12]V. Kourganoff, Compt. Rend. 225, 437 (1947); V. Kourganoff, Ann. Astrophys. 10, 282 (1947).
[13]J. Callaway, R. W. Labahn, R. T. Pu, and W. M. Duxler, Phys. Rev. 168, 12 (1968).
[14]A. Dalgarno and R. W. McCarroll, Proc. Roy. Soc. (London) A237, 383 (1956).
[15]C. J. Kleinman, Y. Hahn, and L. Spruch, Phys. Rev. 165, 53 (1968).
[16]A. Dalgarno, G. W. F. Drake, and G. A. Victor, Phys. Rev. 176, 194 (1968).

PHYSICAL REVIEW A VOLUME 2, NUMBER 1 JULY 1970

Numerical Solution of the Two-Electron Schrödinger Equation

Nicholas W. Winter,*† Arthur Laferrière,‡ and Vincent McKoy
Arthur Amos Noyes Laboratory of Chemical Physics,§
California Institute of Technology, Pasadena, California 91109
(Received 15 January 1970)

Numerical solutions to the S-limit equations for the helium ground state, excited triplet state, and the hydride-ion ground state are obtained with the second and fourth difference approximations. The results for the ground states are superior to previously reported values. The coupled equations resulting from the partial-wave expansion of the exact helium atom wave function are solved giving accurate S, P, D, F, and G limits. The G limit is $-2.903\,51$ a.u., compared to the exact value of the energy of $-2.903\,72$ a.u.

I. INTRODUCTION

It is a well-established approach to the study of electron correlation to analyze the many-electron system as a series of simpler two-electron problems. Sinanoğlu[1] has shown how the first-order equation can be reduced to two-electron pair equations for the many-electron atom or molecule. He also discusses the equation for "exact pairs" which describes the pair correlations beyond first order. Nesbet[2] has been successful in reducing the total wave function and energy for first-row atoms into their Hartree-Fock and two-body components. The general topic of electron correlation is reviewed in Refs. 3 and 4.

We are not concerned here with the derivation of the various pair approximations, but with how to accurately and efficiently solve the resulting equations. There have been two standard approaches in the past, both of which are variational. The first dates back to the early calculations of Hylleraas[5] who used a trial function containing interelectronic coordinates. The unspecified parameters are determined so as to minimize the two-electron energy. This method is capable of high accuracy if enough terms are included, but leads to difficult integrals to evaluate. Indeed, considerable research effort has gone into the study of these integrals themselves. The most successful approach is to use a configuration interaction (CI) trial function. The popularity of this method is due in part to its general applicability. When applied to the pair equations, the CI method obtains the pair energies and properties without dealing directly with a two-electron equation. Instead, the total N-electron wave function is constructed from a set of Slater determinants so as to describe the correlation between a specific pair of electrons, while treating the remaining N-2 electrons in the Hartree-Fock approxi-

mation. The energy is found by diagonalizing the total Hamiltonian in this basis. This is equivalent to solving a Schrödinger equation describing the pair of electrons correlating in the Hartree-Fock field of the remaining N-2 electrons. The principal disadvantage of the CI method is the slow convergence relative to the use of interelectronic coordinates. Schwartz[6,7] has pointed out the disadvantages of using orbital expansions to represent correlated wave functions, with particular attention to the convergence as higher angular configurations are included.

We have chosen an alternative to these approaches by simply solving the equations numerically. Since it is not possible to treat a six-dimensional equation, we first eliminate the angular variables by a partial-wave expansion. Then, the resulting equations for the functional coefficients are solved numerically. The method is not variational and does not necessarily give an upper bound to the two-electron energy. However, once the basic techniques are established, any set of two-variable equations can be solved with high accuracy. This allows one to consider a variety of approximations to the pair equations (pseudopotentials, etc.) without additional complications. The numerical methods are highly computer oriented, since the differential equation is reduced to a set of difference equations which are solved by standard matrix techniques.

In two earlier papers,[8,9] we applied the matrix finite difference (MFD) method to the solution of the S-limit Schrödinger equation and the first-order pair equation for the helium atom. The results were accurate; however, in order to apply the method to excited states of two-electron atoms and to the valence electron pairs in first-row atoms, it was necessary to reexamine the numerical techniques. The most obvious problem originates from the diffuse nature of the wave function describing these electron pairs. This requires that the point at which the solution is required to vanish must be taken further out and, consequently, the number of points needed to obtain an accurate solution becomes unreasonable. Another refinement is needed when considering the solution of exact pair equations. The partial-wave expansion of the exact pair function leads to a set of coupled equations, in contrast to the first-order pairs which give uncoupled equations. The exact-pair functions are solutions of eigenvalue equations, differing from the two-electron atom Schrödinger equation only in the presence of the potential due to the N-2 "core" electrons and orthogonality constraints. In order to solve these, we have to iterate among the equations determining the functional coefficients of the partial-wave expansion. To keep the problem within limits, we must be able to obtain accurate solutions with a small number of points.

We have corrected for the possible diffuse nature of the pair functions by transforming to a new set of variables which are just the square roots of the original variables. In order to guarantee greater accuracy with fewer points, fourth differences have been included in the approximation of the derivatives. Combining both of these modifications with an extrapolation procedure, we have found the S limits for the ground states of helium and the hydride ion. The equations were also solved using both transformed and untransformed coordinates and second differences only. With the three sets of results for each atom, we can compare the effectiveness of the modifications for a tightly bound pair (helium) and a diffuse pair (hydride ion). Finally, we have applied the MFD method to the exact Schrödinger equation for the helium atom using successively higher partial waves up to the G limit. The results proved superior to any previous CI calculation of the angular limits. The properties predicted by the numerical solution compare well to the exact values.

II. PARTIAL-WAVE REDUCTION OF THE TWO-ELECTRON EQUATION

The partial-wave expansion of the solution of the two-electron Schrödinger equation has previously been considered by Luke, Meyerott, and Clendenin[10] for the ^3S state of Li^+. For a spherically symmetric pair of electrons, the exact wave function can be expanded in Legendre polynomials of the cosine of the relative angle between the two electrons,

$$\Psi(r_1 r_2 \theta_{12}) = \sum_{l=0}^{\infty} \psi_l(r_1 r_2) \times \frac{(2l+1)^{1/2}}{4\pi} P_l(\cos\theta_{12}) \,. \tag{1}$$

By substituting this into the equation, we get

$$(-\tfrac{1}{2}\nabla_1^2 - \tfrac{1}{2}\nabla_2^2 + V(r_1) + V(r_2) + 1/r_{12})\,\Psi = E\Psi \,, \tag{2}$$

multiplying both sides by $(2l+1)^{1/2}/4\pi P_l(\cos\theta_{12})$, and integrating over all angular variables, we obtain the lth member of an infinite set of coupled equations for the functional coefficients

$$\left\{-\frac{1}{2}\left[-\frac{1}{r_1^2}\frac{\partial}{\partial r_1}\left(r_1^2\frac{\partial}{\partial r_1}\right)+\frac{1}{r_2^2}\frac{\partial}{\partial r_2}\left(r_2^2\frac{\partial}{\partial r_2}\right)\right]\right.$$
$$\left. + l(l+1)/2r_1^2 + l(l+1)/2r_2^2 + V(r_1) + V(r_2) + M_{ll}\right\}\psi_l(r_1 r_2) = E\cdot\psi_l(r_1 r_2)$$
$$- \sum_{l'\neq l} M_{ll'}\psi_{ll'}(r_1 r_2) \,, \tag{3}$$

where $M_{ll'} = \sum_{k=|l-l'|}^{l+l'} C^k(l0, l'0)\, \frac{r_<^k}{r_>^{k+1}}$,

$r_< = \min(r_1, r_2)$, $\quad r_> = \max(r_1, r_2)$,

and $C^k(l0, l'0) = \frac{1}{2}[(2l+1)(2l'+1)]^{1/2}$

$\times \int (P_l(\cos\theta_{12})\, P_k(\cos\theta_{12})\, P_{l'}(\cos\theta_{12}))\, d(\cos\theta_{12})$.

Up to this point, we have not made any approximations, although it is clearly an impossible task to solve an infinite set of coupled equations. The expansion is usually truncated when the energy is determined to the desired accuracy. When using the MFD method it is convenient, but not necessary, to begin by solving the S limit ($l=0$ partial wave only) and then use this as an initial guess to determine the P limit ($l=0, 1$ partial waves only), and so forth. After two partial waves, the addition of further terms to the expansion has a small effect on the known functional coefficients, and the iterative method of solving the coupled equations converges extremely rapidly. Therefore, the slow convergence of the partial-wave expansion pointed out by Schwartz[7] is not a serious drawback.

It is easy to show that a similar reduction of the Schrödinger equation can be made for pairs that are not spherically symmetric. The main difference appears in the angular integrals which couple the equations together. Also the nonlocal potentials which occur in the Hartree-Fock pair equations offer little complication since the equations already contain nonhomogeneous terms. The numerical techniques needed to solve these equations are presented in Sec. III.

III. REVIEW OF FINITE DIFFERENCE METHOD

The second derivative can be expanded in terms of differences as follows:

$$\left(\frac{\partial^2\psi}{\partial r^2}\right)_{r=r_0} = \frac{1}{h^2}\left(\delta_0^2 - \tfrac{1}{12}\delta_0^4 + \tfrac{1}{90}\delta_0^6 - \cdots\right), \qquad (4)$$

where

$$\begin{aligned}
\delta_0^2 &= \psi(r_0+h) - 2\psi(r_0) + \psi(r_0-h)\,,\\
\delta_0^4 &= \psi(r_0+2h) - 4\psi(r_0+h) + 6\psi(r_0)\\
\delta_0^6 &= \psi(r_0+3h) - 6\psi(r_0+2h) + 15\psi(r_0+h)\\
&\quad - 20\psi(r_0) + 15\psi(r_0-h)\\
&\quad - 6\psi(r_0-2h) + \psi(r_0-3h)\,, \qquad (5)
\end{aligned}$$

and h is the grid size.[11] The first approximation to the second derivative is just $\partial^2\psi/\partial r^2 \sim (1/h^2)\,\delta^2$. In order to find the difference error, we expand the second difference in terms of derivatives

$$\frac{1}{h^2}\delta_0^2 = \left(\frac{\partial^2\psi}{\partial r^2}\right)_0 + \tfrac{1}{12}h^2\left(\frac{\partial^4\psi}{\partial r^4}\right)_0 + \tfrac{1}{360}h^4\left(\frac{\partial^6\psi}{\partial r^2}\right)_0 + \cdots\,, \qquad (6)$$

and as a consequence of choosing central differences, the error contains only even powers of h. Bolton and Scoins[12] have shown that the energy found with a grid size h can be expressed as a power series of the form

$$E(h) = E(0) + C_2h^2 + C_4h^4 + C_6h^6 + \cdots\,, \qquad (7)$$

where $E(0)$ is the exact energy corresponding to $h=0$. For most two-dimensional equations, it is not possible to use enough points to compete with the accuracy of variational methods, therefore, (7) is used to extrapolate the energies found at several grid sizes to the exact value.[13]

Fox[14] has argued that a substantial amount of the difference error can be eliminated by including the next term in the difference expansion of the derivative in the MFD equations. The difficulty in using fourth differences is satisfying the boundary conditions. The usual conditions are to require $r\psi(r)$ to vanish at $r=0$ and $r=r_{\max}$, where $r_{\max}$ approximates infinity. The fourth difference of $\psi(r)$ at $r=h$ requires that we know the function at $r=-h$, and therefore introduces uncertainties into the MFD equations. A similar difficulty occurs at the other boundary. One solution of this problem is to extract the asymptotic behavior of $\psi(r)$ at $r=0$ and $r=\infty$ from the differential equation and use this to relate the unknown values of $\psi(r)$ outside the defined grid to the values within. This is the approach we have taken for the first-order pair equations; however, for the eigenvalue equations, it is simpler to replace the fourth difference approximation at the boundary with the usual second difference approximation. This does not appreciably affect the accuracy when combined with the coordinate transformation to be discussed later.

Unfortunately, the fourth difference approximation does not sufficiently reduce the difference error to be used without extrapolation. The approximation does allow accurate results to be obtained from relatively few grids. These various methods are illustrated for the S-limit equation in Sec. IV.

IV. SOLUTION OF THE S-LIMIT EQUATION

Truncating the partial-wave expansion at $l=0$, we then obtain the following equation for the two-electron atom,

$$\left(-\frac{\frac{1}{2}\partial^2}{\partial r_1^2} - \frac{\frac{1}{2}\partial^2}{\partial r_2^2} - \frac{z}{r_1} - \frac{z}{r_2} + \frac{1}{r_>}\right)u_0(r_1r_2) = Eu_0(r_1r_2)\,, \qquad (8)$$

where $u_0(r_1r_2) = r_1r_2\psi_0(r_1r_2)$. If the derivatives are replaced by the second difference approximation,

TABLE I. S-limit energy of the helium-atom ground state.

Grid size	Initial energies (a.u.)					
9/20	−2.417 777 93					
	−2.782 694 71					
25	−2.549 147 97	−2.860 638 37				
	−2.825 996 74	−2.876 028 34				
30	−2.633 740 65	−2.871 003 04	−2.878 624 31			
	−2.848 040 64	−2.877 975 31	−2.878 986 31			
35	−2.690 595 75	−2.875 251 77	−2.878 914 80	−2.879 026 36		
	−2.859 945 51	−2.878 624 84	−2.879 019 95	−2.879 027 78		
40	−2.730 287 10	−2.877 125 69	−2.878 993 67	−2.879 027 59	−2.879 030 50	
	−2.866 732 74	−2.878 860 89	−2.879 026 01	−2.879 030 20		
45	−2.758 923 84	−2.878 010 64	−2.879 016 38	−2.879 029 75		
	−2.870 792 79	−2.878 953 40	−2.879 028 82			
50	−2.789 238 40	−2.878 454 74	−2.879 024 59			
	−2.873 325 66	−2.878 992 95				
55	−2.796 344 90	−2.878 690 21				
	−2.874 964 83					
60	−2.808 902 25					

(8) is transformed to a set of linear equations of the form

$$\underline{D}\,\underline{u} = E\underline{u} \ , \tag{9}$$

where $\underline{D}$ is a symmetric-banded matrix with nonzero off-diagonal elements in only two superdiagonals and two subdiagonals. The eigenvectors at $\underline{D}$ represent the ground and excited states of the two-electron equation and would be exact if we used an infinite number of grid points and satisfied the correct boundary conditions. Since we are usually satisfied with the lowest state, and possibly a few excited states, a finite number of points are employed and a reasonable radial cutoff is chosen to approximate the boundary conditions.

We have solved the S-limit equation for the first two states of the helium atom and for the ground state of the hydride ion using the second difference approximation. The radial cutoff for the ground state of helium was taken at 9 a.u. and for the excited state at 20 a.u. For the hydride ion, the solution was required to vanish at 25 a.u. Equation (8) was solved for several grid sizes and the eigenvalues extrapolated using the polynomial representation of the difference error. From (7), we see that two eigenvalues are needed to eliminate the h^2 term, three for the h^2 and h^4 terms, etc. We have done this for the three states and present the results in Tables I–III.

TABLE II. The S-limit energy of the helium-atom triplet excited state.

Grid size	Initial energies (a.u.)			
20/50	−1.921 557 42			
	−2.145 824 78			
75	−2.046 150 40	−2.171 854 06		
	−2.165 346 74	−2.174 111 34		
100	−2.098 298 80	−2.173 750 17	−2.174 254 68	
	−2.170 724 94	−2.174 238 75		
125	−2.124 372 21	−2.174 116 61		
	−2.172 609 20			
150	−2.139 111 29			

The extrapolation of the S limit for the helium ground state predicts an energy of −2.879 031 a.u., with an uncertainty in the last figure. The previous best limit was found by Davis[15] and by Schwartz[7] to be −2.879 028 a.u. Table I shows the extrapolated values found using successively more of the initial energies to be converging from above. Thus the best extrapolant should be an upper bound to the true S limit. This value falls within the error bounds on Davis's predicted limit.

The results for the ^3S state of helium and the ground state of the hydride ion are less satisfactory. Davis[15,16] places the S limits of these states at −2.174 265 2 a.u. and −0.514 494 0 a.u., respectively. The MFD method is more difficult for these states because of their large radial extent. To achieve the accuracy that we have, it was necessary to diagonalize a matrix as large as 22 500 by 22 500 for the ^3S state and about 15 000 by 15 000 for the hydride ion.

In order to avoid this problem, we made the following coordinate transformation:

$$r_1 = x_1^2 \ , \quad r_2 = x_2^2 \ , \tag{10}$$

TABLE III. S-limit energy of the hydride ion on the linear grid.

Grid size	Initial energies (a.u.)				
25/50	−0.482 652 39				
75	−0.499 282 47	−0.512 586 53	−0.514 387 70	−0.514 470 16	
100	−0.505 694 01	−0.513 937 41	−0.514 456 95		
125	−0.508 781 34	−0.514 269 92			

and solved the Schrödinger equation on an evenly spaced grid in x_1 and x_2. The effect of this is to give a dense distribution of points near the nucleus and a sparse distribution in the tail regions, as viewed in the untransformed system. Not only is the radial cutoff less important in the new system, but since this is a more optimum distribution of points for our problem, we can use fewer points without losing accuracy.

Substituting the transformation into (3), the derivatives become

$$\frac{1}{r^2}\frac{\partial}{\partial r}\left(r^2\frac{\partial}{\partial r}\right)=\frac{1}{4r}\left(\frac{\partial^2}{\partial X^2}-\frac{1}{X}\frac{\partial}{\partial X}\right). \qquad (11)$$

The first derivative is eliminated by the transformation

$$\psi_0(x_1x_2)=u_0(x_1x_2)/x_1^{3/2}x_2^{3/2},$$

which leads to the following equation for $U_o(X_1X_2)$:

$$\left\{-\frac{1}{2}\left[\frac{1}{4r_1}\left(\frac{\partial^2}{\partial x_1^2}-\frac{3}{4r_1}\right)+\frac{1}{4r_2}\left(\frac{\partial^2}{\partial x_2^2}-\frac{3}{4r_2}\right)\right]-\frac{z}{r_1}-\frac{z}{r_2}+\frac{1}{r}>\right\}u_o(x_1x_2)\equiv Eu_o(x_1x_2). \qquad (12)$$

This equation was solved for the hydride ion with a 25 a.u. radial cutoff (5 a.u. on the square-root grid) using grids ranging from 25 to 50 strips. The results were extrapolated to $E=-0.514497$ a.u. and were converging from below. Representation of the difference error using only even powers of h was not as efficient for the new coordinates, giving an energy of -0.514557 a.u., also converging from below. Therefore a polynomial containing both even and odd powers, but leading off with h^2, was used. The square-root grid reduced the computation time by a factor of 7 for this case.

TABLE IV. S-limit energies for the helium atom and the hydride ion on the square-root grid.

Grid size	Second differences	Fourth differences
	(helium)	
3/20	−2.946 122 43	−2.916 524 55
25	−2.923 134 14	−2.902 536 97
30	−2.910 423 77	−2.895 141 53
35	−2.902 606 78	−2.890 761 50
40	−2.897 435 38	−2.887 954 43
45	−2.893 826 42	−2.886 047 78
50	−2.891 202 57	−2.884 693 60
55	−2.889 232 04	−2.883 697 18
60	−2.887 712 61	−2.882 942 65
	(Hydride)	
$(30)^{1/2}/25$		−0.522 003 14
30	−0.523 875 59	−0.519 603 70
35	−0.521 513 23	−0.518 196 44
40	−0.519 961 46	−0.517 300 55
45	−0.518 883 29	−0.516 694 99
50	−0.518 101 67	−0.516 266 49
55	−0.517 515 82	−0.515 952 12
60	−0.517 064 69	−0.515 714 63

TABLE V. Polynomial fits for the helium atom S limit.[a]

Grids used in the polynomial fit	$h^2h^4h^6\cdots$	$h^2h^3h^4\cdots$	$h^2h^4h^5\cdots$
		(Second differences)	
(20-25)	−2.882 266 07	−2.882 266 07	−2.882 266 07
(20-30)	−2.880 952 96	−2.880 661 16	−2.880 952 96
(20-35)	−2.880 070 81	−2.879 548 72	−2.879 970 00
(20-40)	−2.879 681 14	−2.879 302 72	−2.879 559 36
(20-45)	−2.879 469 67	−2.879 183 52	−2.879 352 27
(20-50)	−2.879 342 22	−2.879 122 50	−2.879 237 38
(20-55)	−2.879 260 80	−2.879 093 07	−2.879 171 24
(20-60)	−2.879 200 98	−2.879 035 06	−2.879 113 56
		(Fourth differences)	
(20-25)	−2.877 670 16	−2.877 670 16	−2.877 670 16
(20-30)	−2.878 864 55	−2.879 129 97	−2.878 864 55
(20-35)	−2.878 981 18	−2.879 050 20	−2.878 994 51
(20-40)	−2.879 012 72	−2.879 040 11	−2.879 022 57
(20-45)	−2.879 022 53	−2.879 031 81	−2.879 027 66
(20-50)	−2.879 025 00	−2.879 025 23	−2.879 026 45
(20-55)	−2.879 026 82	−2.879 031 94	−2.879 028 96
(20-60)	−2.879 028 86	−2.879 036 98	−2.879 032 36

[a]Square-root grid with a 9 a.u. cutoff.

In an effort to improve the MFD method further, the fourth difference approximation was used to resolve the equations for helium and the hydride ion on the square-root grid. The cutoff for helium was kept at 9 a.u., but the cutoff for the hydride ion was taken at 30 a.u. The energies obtained using both second and fourth difference approximations are given in Table IV. While the fourth difference results are improved, the accuracy is not sufficient to be used without extrapolation. In order to find the appropriate extrapolation method, the energies were fitted to various polynomials in the grid size using successively finer grids. By studying the trends in the extrapolants and the coefficients of the power series, we can determine the most efficient form to represent the difference error. The results for the polynomial fits of the helium energies are given in Table V.

The best representation of the difference error

TABLE VI. Polynomial fits for the hydride ion S limit.[a]

Grids used in the polynomial fit	$h^2h^4h^6\cdots$	$h^2h^3h^4\cdots$	$h^2h^4h^5\cdots$
		(Second differences)	
(30-35)	−0.514 597 13	−0.514 597 13	−0.514 597 13
(30-40)	−0.514 790 82	−0.514 745 69	−0.514 790 82
(30-45)	−0.514 663 52	−0.514 577 09	−0.514 646 55
(30-50)	−0.514 604 82	−0.514 538 88	−0.514 583 22
(30-55)	−0.514 572 61	−0.514 522 80	−0.514 551 57
(30-60)	−0.514 547 15	−0.514 487 62	−0.514 521 28
		(Fourth differences)	
(25-30)	−0.514 150 43	−0.514 150 43	−0.514 150 43
(25-35)	−0.514 454 61	−0.514 527 03	−0.514 454 61
(25-40)	−0.514 479 61	−0.514 495 63	−0.514 482 74
(25-45)	−0.514 487 79	−0.514 495 84	−0.514 490 60
(25-50)	−0.514 489 98	−0.514 491 72	−0.514 491 20
(25-55)	−0.514 491 88	−0.514 496 35	−0.514 493 70
(25-60)	−0.514 491 72	−0.514 487 20	−0.514 490 81

[a]Square-root grid with a 30 a.u. cutoff.

TABLE VII. Comparison of the properties predicted by the S-limit wave functions to the radial configuration interaction and Hartree-Fock results for He and H^-.

Property	Helium (^1S) FD	RCI[a]	HF	Hydride ion FD	RCI[b]	HF[c]
E	−2.879 03	−2.879 00	−2.861 68	−0.514 49	−0.514 46	−0.488 0
V	−5.758 1	−5.758 0	−5.723 8	−1.029 0	−1.028 9	···
V/E	2.000 0	2.000 0	2.000 0	2.000 1	2.000 0	···
$\langle 1/r_{12}\rangle$	0.986 7	0.986 7	1.025 8	0.298 3	(0.297 3)	···
$\langle 1/r_1+1/r_2\rangle$	3.372 4	3.372 4	3.374 8	1.327 3	···	1.371 4
$\langle r_1+r_2\rangle$	1.869 0	1.868 8	1.854 6	6.207 9	6.207	5.007 8
$\langle r_1^2+r_2^2\rangle$	2.422 1	2.420 6	2.369 6	34.518	34.44	18.821

[a]The basis set for the RCI calculation consisted of $1s$, $2s$, and $3s$ Slater orbitals with $\zeta = 3.7530$ and $1s'$ and $2s'$ orbitals with $\zeta = 1.5427$.

[b]W. A. Goddard, J. Chem. Phys. 48, 1008 (1968); the value in parenthesis is from a G_1 calculation.

[c]K. E. Baynard, J. Chem. Phys. 48, 2121 (1968).

for the second difference approximation is given by the polynomial containing a cubic term in h. For the fourth difference results the polynomial

$$E(h) = E(0) + C_2h^2 + C_4h^4 + C_5h^5 + C_6h^6 + \cdots \quad (13)$$

appears to give the best extrapolant, but by eliminating odd powers entirely we obtain accurate results and uniform convergence from above. We should point out that while the error in the fourth difference approximation leads off as h^4, using second differences at the boundary introduces the h^2 term. Table VI gives the equivalent information for the hydride ion. The fourth difference approximation predicts an S-limit energy of −0.514 491 ±0.000 001 a.u., which is within the error bounds of Davis's result.

Even though the wave functions found by the MFD method are only known at discrete points, there is no problem extracting the same information from them that a variational solution can yield. In fact, the numerical solutions are generally of a higher quality over all regions of space than the variational functions. This is illustrated by the local energy which agrees with the eigenvalue to six or more decimal places at every grid point. Properties are easily calculated by quadrature methods which amount to nothing more than double summations. These are then extrapolated in the same manner as the energy.

We have calculated several properties from the fourth difference S-limit functions for helium and the hydride ion, and compare them to the radial CI and Hartree-Fock values in Table VII. The agreement is very good except for $\langle r_1^2+r_2^2\rangle$, which indicates that more diffuse basis functions were needed in the radial CI calculations.

Contour and perspective plots of the two helium states and the hydride ion ground state are given in Fig. 1. We have plotted the square of the functions $u_o(r_1r_2)$ in each case. The contour plots show the regions r_1, $r_2 \leq 4.5$ a.u. for the ^1S state of helium, r_1, $r_2 \leq 10$ a.u. for the ^3S state, and r_1, $r_2 \leq 12.5$ a.u. for the hydride ion. The nucleus is positioned at the lower left-hand corner and the constant contour increment is given in the upper right-hand corner. The lowest contour is labeled. In the 3-D plots the regions shown are r_1, $r_2 \leq 7.5$ a.u. for the helium ^1S state, r_1, $r_2 \leq 13.3$ a.u. for the ^3S state, and r_1, $r_2 \leq 18.7$ a.u. for the hydride ion. Figure 2 gives the viewer's orientation for these plots. The functional axis has the same scale in each case, so that the heights of the surfaces can be compared. The contour plot for the hydride ion shows the minimum in the solution along the line $r_1 = r_2$. The helium atom shows a similar feature for large radial distances, but only slightly. This minimum is not present for the Hartree-Fock wave function, which does not predict a stable ground state for the ion.

While including radial correlation relative to the Hartree-Fock model leads to a stable ion, the S-limit functions give unreasonable values for some properties. The exact value of $\langle r_1^2+r_2^2\rangle$ is 23.827 a.u.,[17] which is about $\frac{2}{3}$ of the S-limit value. If we include the higher partial waves in our expansion of the exact solution, the S wave contracts and the expectation values approach the exact results. This is illustrated for the helium atom in Sec. V.

V. SOLUTION OF THE COUPLED PARTIAL-WAVE EQUATIONS FOR THE HELIUM ATOM

The MFD method was applied to the sets of coupled equations that result when (1) is truncated at $l = 1, 2, 3$, and 4. We decided to use the second difference approximation on the linear grid with a 9-a.u. cutoff since this proved to be very accurate for the S limit. For a more diffuse state the square root grid would have been used.

The extrapolation tables for the angular limits

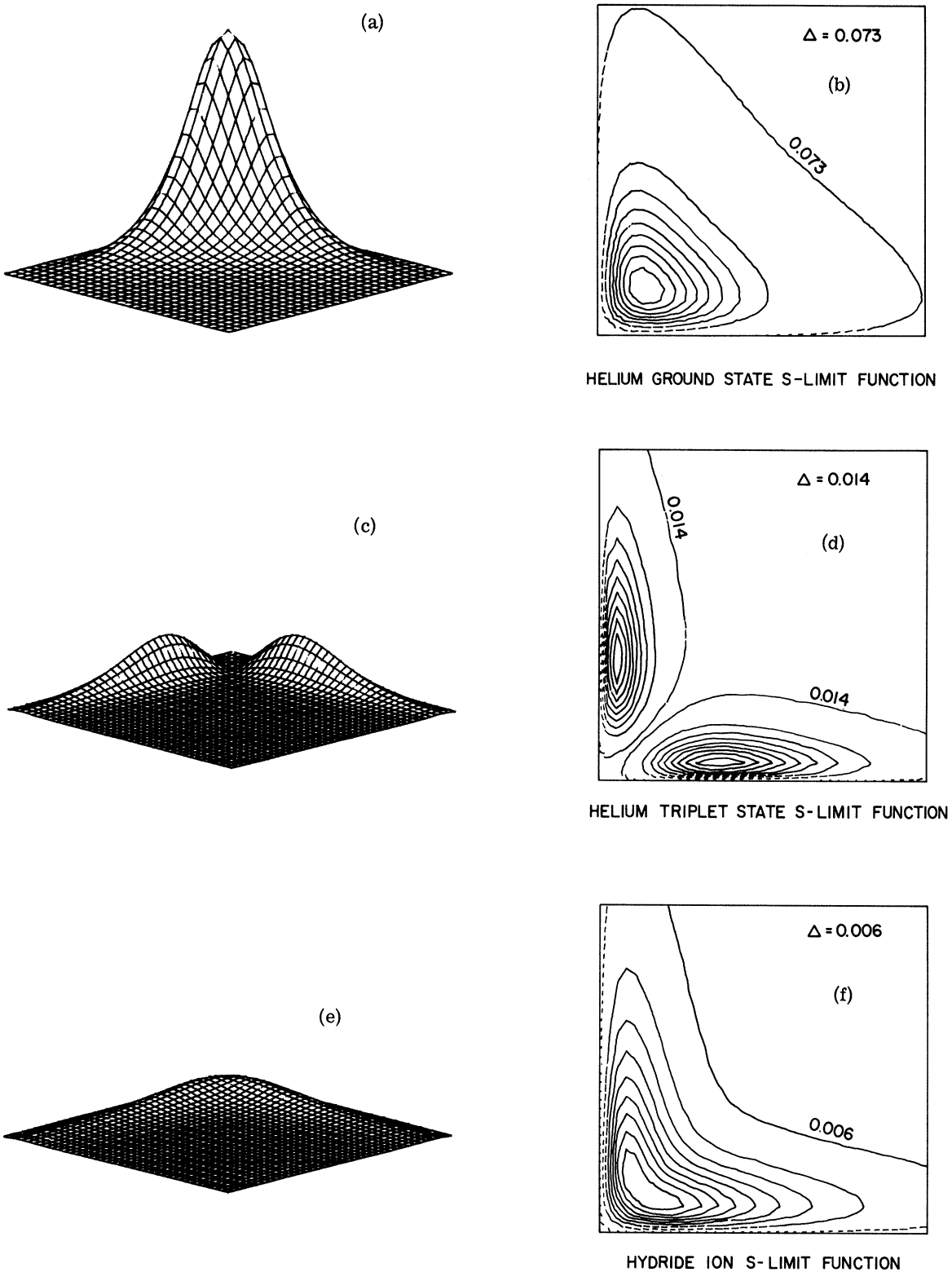

FIG. 1. Contour and perspective plots of the S limit for the $(1s^2)\,^1S$ and $(1s2s)\,^3S$ states of helium and the $(1s^2)\,^1S$ state of the hydride ion.

TABLE VIII. Extrapolation tables for the angular limits of the helium atom.

Grid size				
		P limit		
9/20	−2.449 610 31			
	−2.803 933 59			
25	−2.577 166 69	−2.881 793 94		
	−2.847 189 34	−2.897 463 39		
30	−2.659 673 61	−2.892 346 83	−2.900 114 14	
	−2.869 307 29	−2.899 451 45	−2.900 475 91	
35	−2.715 290 71	−2.896 676 21	−2.900 404 45	−2.900 513 10
	−2.881 281 20	−2.900 110 32	−2.900 507 15	
40	−2.754 194 73	−2.898 584 05	−2.900 481 48	
	−2.888 116 89	−2.900 347 86		
45	−2.782 301 85	−2.899 483 59		
	−2.892 208 90			
50	−2.803 184 19			
		D limit		
9/20	−2.453 150 95			
	−2.806 424 76			
25	−2.580 329 52	−2.884 068 03		
	−2.849 559 91	−2.899 709 53		
30	−2.662 594 36	−2.894 602 10	−2.902 355 48	
	−2.871 621 39	−2.901 693 99	−2.902 719 70	
35	−2.718 050 51	−2.898 923 72	−2.902 647 76	−2.902 759 87
	−2.883 566 16	−2.902 353 39	−2.902 753 44	
40	−2.756 843 24	−2.900 829 09	−2.902 727 02	
	−2.890 386 08	−2.902 592 51		
45	−2.784 870 75	−2.901 728 44		
	−2.894 469 33			
50	−2.805 694 48			
		F limit		
9/20	−2.454 238 36			
	−2.807 141 75			
25	−2.581 283 58	−2.884 659 52		
	−2.850 207 18	−2.900 266 97		
30	−2.663 454 68	−2.895 170 66	−2.902 904 73	
	−2.872 230 11	−2.902 245 29	−2.903 268 75	
35	−2.718 844 08	−2.899 481 76	−2.903 196 84	−2.903 311 88
	−2.884 152 71	−2.902 903 15	−2.903 304 98	
40	−2.757 588 29	−2.901 382 54	−2.903 277 95	
	−2.890 959 55	−2.903 143 02		
45	−2.785 579 79	−2.902 280 38		
	−2.895 035 05			
50	−2.806 376 29			
		G limit		
9/20	−2.454 719 02			
	−2.807 446 77			
25	−2.581 701 01	−2.884 890 07		
	−2.850 470 82	−2.900 471 29		
30	−2.663 825 12	−2.895 383 54	−2.903 100 98	
	−2.872 468 89	−2.902 443 55	−2.903 463 46	
35	−2.719 179 59	−2.899 685 74	−2.903 391 86	−2.903 505 56
	−2.884 376 26	−2.903 099 17	−2.903 498 82	
40	−2.757 897 56	−2.901 582 09	−2.903 472 08	
	−2.891 173 63	−2.903 337 83		
45	−2.785 869 08	−2.902 477 52		
	−2.895 243 03			
50	−2.806 650 13			

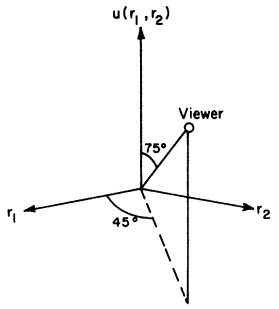

FIG. 2. Viewer's orientation for the perspective plots.

are given in Table VIII. The results converge from above so that the best extrapolants should be upper bounds to the true limit. These are compared to various CI calculations in Table IX. We note that the numerical G limit is superior to each of the other calculations. Tycko, Thomas, and King[18] were only able to obtain an energy of $-2.903\,44$ a. u. using 15 partial waves. This illustrates the difficulty in representing the functional coefficients with orbital products for the higher partial waves. As pointed out by Schwartz,[7]

TABLE IX. Comparison of the angular limits for the helium atom.

Limit	Numerical		Weiss[a]		Nesbet[b]		Tycko[c]	
S	$-2.879\,03$	$-0.021\,48$	$-2.878\,96$	$-0.021\,43$	$-2.878\,87$	$-0.021\,42$	$-2.878\,92$	$-0.021\,52$
P	$-2.900\,51$	$-0.002\,25$	$-2.900\,39$	$-0.002\,19$	$-2.900\,29$	$-0.002\,09$	$-2.900\,44$	$-0.002\,25$
D	$-2.902\,76$	$-0.000\,55$	$-2.902\,58$	$-0.000\,49$	$-2.902\,38$	$-0.000\,38$	$-2.902\,69$	$-0.000\,54$
F	$-2.903\,31$	$-0.000\,20$	$-2.903\,07$	$-0.000\,13$	$-2.902\,76$	...	$-2.903\,23$	$-0.000\,14$
G	$-2.903\,51$		$-2.903\,20$		...		$-2.903\,37$	
Exact[d]	$-2.903\,72$							

[a]A. W. Weiss, Phys. Rev. 122, 1826 (1961).
[b]R. K. Nesbet and R. E. Watson, Phys. Rev. 110, 1073 (1958).
[c]D. H. Tycko, L. H. Thomas, and K. M. King, Phys. Rev. 109, 369 (1958).
[d]C. L. Pekeris, Phys. Rev. 115, 1216 (1959).

TABLE X. Electron repulsion matrix.

l	$\langle l\|1/r_{12}\|0\rangle$	$\langle l\|1/r_{12}\|1\rangle$	$\langle l\|1/r_{12}\|2\rangle$	$\langle l\|1/r_{12}\|3\rangle$	$\langle l\|1/r_{12}\|4\rangle$
0	0.988 972	$-0.020\,919$	$-0.002\,646$	$-0.000\,695$	$-0.000\,255$
1	$-0.020\,919$	0.004 461	0.000 428	0.000 107	0.000 038
2	$-0.002\,646$	0.000 428	0.000 225	0.000 041	0.000 014
3	$-0.000\,695$	0.000 107	0.000 041	0.000 033	0.000 008
4	$-0.000\,255$	0.000 038	0.000 014	0.000 008	$0.000\,007_8$
$\sum_l$	0.964 457	$-0.015\,885$	$-0.001\,938$	$-0.000\,506$	$-0.000\,187$

TABLE XI. Partial-wave analysis of the energy for helium (a.u.).

l	T_l	$V_{l\,\mathrm{nuc}}$	V_l	E_l
0	2.877 088	$-6.732\,944$	$-5.768\,487$	$-2.891\,399$
1	0.022 998	$-0.018\,653$	$-0.034\,538$	$-0.011\,490$
2	0.002 222	$-0.000\,810$	$-0.002\,748$	$-0.000\,527$
3	0.000 542	$-0.000\,110$	$-0.000\,615$	$-0.000\,073$
4	0.000 194	$-0.000\,024$	$-0.000\,211$	$-0.000\,017$
$\sum_l$	2.903 044	$-6.752\,541$	$-5.806\,599$	$-2.903\,506$

TABLE XII. Partial-wave analysis of expectation values for helium.

l	$\langle r_1+r_2\rangle_l$	$\langle r_1^2+r_2^2\rangle_l$	$\langle 1/r_1+1/r_2\rangle_l$	$\sum_{l'}\langle 1/r_{12}\rangle_{ll'}$
0	1.850 14	2.376 18	3.366 47	0.964 46
1	0.008 37	0.010 64	0.009 33	0.015 89
2	0.000 39	0.000 50	0.000 41	0.001 94
3	0.000 06	0.000 07	0.000 06	0.000 51
4	$0.000\,01_3$	$0.000\,01_6$	$0.000\,01_2$	0.000 19
$\sum_l$	1.858 97	2.387 41	3.376 27	0.945 94
Exact[a]	1.858 94	2.386 97	3.376 63	0.945 82

[a]C. L. Pekeris, Phys. Rev. 115, 1216 (1959).

this led to the erroneous conclusion that the majority of the error was in the S limit and that the contribution from the higher waves could be neglected. The CI calculations generally do worse for the higher angular limits, because to keep the calculations from becoming intractable, fewer configurations are used to represent the functional coefficients. The MFD method actually becomes easier for these equations since the coefficients have less and less amplitude and are concentrated nearer the line $r_1 = r_2$.

The energy can be expressed in the form

$$E = \sum_l E_l , \tag{14}$$

where

$$E_l = \langle l \mid -\tfrac{1}{2}\nabla_1^2 - \tfrac{1}{2}\nabla_2^2 - z/r_1 - z/r_2 \mid l\rangle + \sum_l \sum_k \langle l \mid r_<^k / r_>^{k+1} \mid l'\rangle C^k(lo, l'o) = T_l + V_l .$$

Using the G-limit solution, we have calculated the

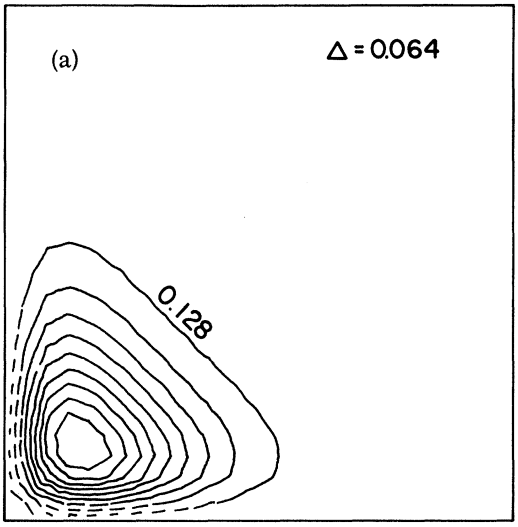

S-PARTIAL WAVE FOR THE HELIUM ATOM

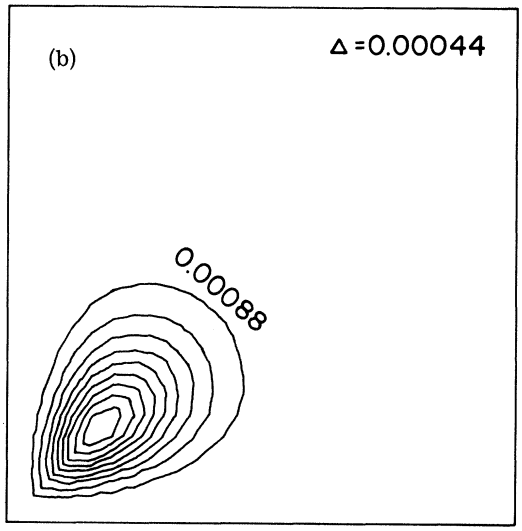

P-PARTIAL WAVE FOR THE HELIUM ATOM

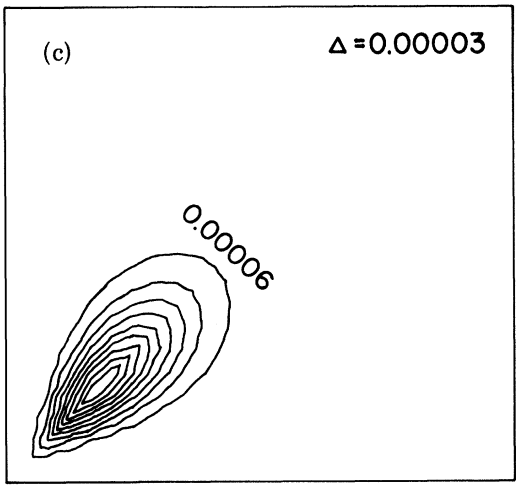

D-PARTIAL WAVE FOR THE HELIUM ATOM

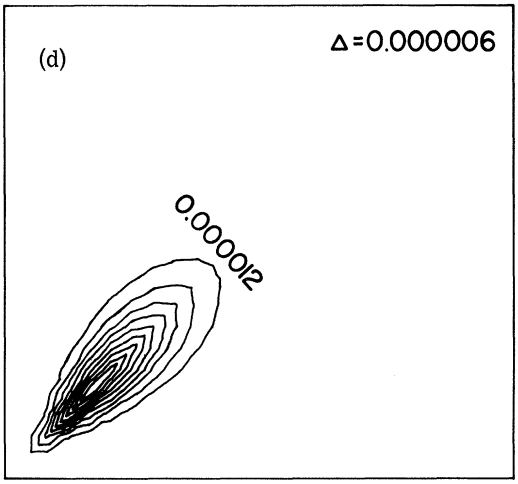

F-PARTIAL WAVE FOR THE HELIUM ATOM

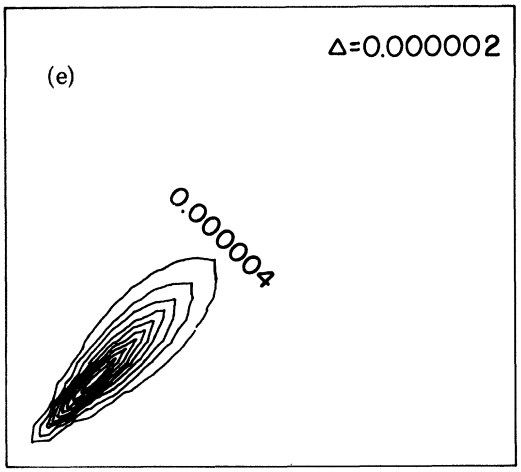

G-PARTIAL WAVE FOR THE HELIUM ATOM

FIG. 3. Contour plots of the functional coefficients for the helium *G*-limit wave function.

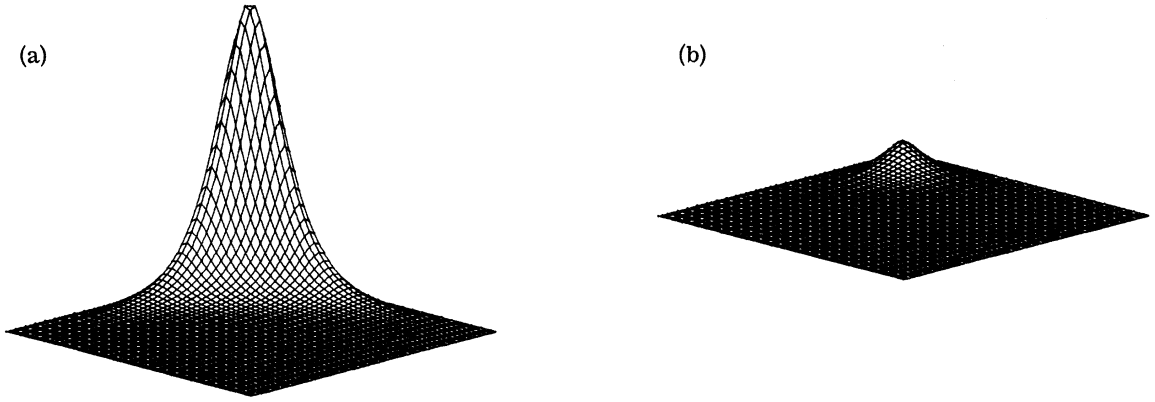

FIG. 4. Perspective plots of the S- and P-wave functional coefficients for the helium atom.

different terms in this expression. The electron repulsion matrix elements $\sum_k \langle l \mid r_<^k / r_>^{k+1} \mid l' \rangle \times C^k(lo, l'o)$ are presented in Table X and the energy analysis in Table XI. These results illustrate the small but important effects the higher partial waves have on the energy. Several properties were studied in the same manner and compared to the exact values in Table XII. The accuracy is very good, being about four decimal places in every case except for $\langle r_1^2 + r_2^2 \rangle$. The value is still too large and would improve if more partial waves were used.

The contour plots of each functional coefficient for the G limit are given in Fig. 3. Again the squares of the functions $u_i(r_1 r_2)$ are plotted over the region r_1, $r_2 \leq 4.5$ a. u. The peakedness of the higher partial waves about the line $r_1 = r_2$ is quite evident. Since the amplitude of the functions for $l > 0$ is negative, their effect is to reduce the electron density in this region. Figure 4 gives the perspective plots of the S and P waves using the same scale along the functional axis. By integrating over the radial variables, we found the volume under the P-wave surface to be 0.4% of that under the S wave. The remaining waves were too small to be shown with this scale, but the same integration showed the D wave to be 5% of the P wave and the F wave about 17% of the D wave.

VI. DISCUSSION

The results presented here demonstrate that the numerical solution of partial differential equations can give accuracy competitive with variational methods. The values found for the S limits of helium and the hydride ion are superior to any previous calculation and agree well with the predicted limits given by Davis. More importantly, the same accuracy was found when the coupled equations were solved for helium. The equations describing the pair correlations in atoms offer virtually no new considerations once they are derived. The same program which was used for the helium atom has been used to calculate the valence pair correlation energy for beryllium, and the MFD method has been applied to the first-order hydrogenic pair equations for lithium. The results were consistently accurate in all cases.

The calculations reported here were carried out on the CDC 6600 and IBM 360-75 computers. The IBM 360-75 results were found using double-precision arithmetic to avoid round-off errors.

---

*Work based on a thesis submitted by N. W. Winter in partial fulfillment of the requirements for the degree of Doctor of Philosophy in Chemistry, California Institute of Technology.

†Present address: Battelle Memorial Institute, Columbus Ohio.

‡Present address: Chemistry Department, Rhode Island College, Providence, R.I.

§Contribution No. 4043.

[1]O. Sinanoğlu, J. Chem. Phys. 36, 3198 (1962).

[2]R. K. Nesbet, Phys. Rev. 175, 2 (1968).

[3]O. Sinanoğlu, Advan. Chem. Phys. 6, 315 (1964).

[4]R. K. Nesbet, Advan. Chem. Phys. 9, 321 (1965).

[5]E. A. Hylleraas, Z. Phyzik 54, 347 (1929).

[6]C. Schwartz, Methods Comp. Phys. 2, 241 (1963).

[7]C. Schwartz, Phys. Rev. 126, 1015 (1962).

[8]N. W. Winter, D. Diestler, and V. McKoy, J. Chem. Phys. 48, 1879 (1968).

[9]V. McKoy and N. W. Winter, J. Chem. Phys. 48, 5514 (1968).

[10]P. Luke, R. Meyerott, and W. Clendenin, Phys. Rev. 85, 401 (1952).

[11]The grid size is given by $h = r_n/(n-1)$, where r_n is the last grid point and $n-1$ is the number of strips in the grid.

[12]H. C. Bolton and H. I. Scoins, Proc. Cambridge Phil. Soc. 53, 150 (1956).
[13]This is sometimes called Richardson extrapolation. L. Richardson and J. Gaunt, Trans. Roy. Soc. (London) A226, 299 (1927).
[14]L. Fox, *Numerical Solution of Two-Point Boundary Problems* (Oxford U.P., London, 1957).
[15]H. L. Davis, J. Chem. Phys. 39, 1827 (1963).
[16]H. L. Davis, J. Chem. Phys. 39, 1183 (1963).
[17]C. L. Pekeris, Phys. Rev. 126, 1470 (1962).
[18]D. H. Tycko, L. H. Thomas, and K. M. King, Phys. Rev. 109, 369 (1958).

PHYSICAL REVIEW A VOLUME 2, NUMBER 1 JULY 1970

Theory of Stokes Pulse Shapes in Transient Stimulated Raman Scattering*

R. L. Carman, F. Shimizu, C. S. Wang, and N. Bloembergen
Division of Engineering and Applied Physics, Harvard University, Cambridge, Massachusetts 02138
(Received 16 January 1970)

The theory of transient stimulated Raman scattering has been extended to include an arbitrary shape of the laser pump pulse. It is shown that the maximum Stokes gain depends on the total energy content per unit area of the pump pulse, and not on the instanteous intensity for an exciting pulse of short duration. The Stokes pulse has a leading edge which rises sharply to a maximum, where the maximum occurs with some delay with respect to the maximum of the pump pulse. The trailing edge follows the decay of the pump. In a nondispersive medium, the gain is not reduced by frequency broadening of the laser output, while in a dispersive medium, considerable gain reduction is expected. Numerical results for various laser-pulse shapes and spectral distributions are presented.

I. INTRODUCTION

Several experimental investigations of the stimulated Raman effect induced by a train of picosecond pulses from a mode-locked laser have recently been reported.[1-6] It has been demonstrated[6] that the Stokes light is emitted in the forward direction in picosecond pulses with a duration which is equal to or shorter than the laser pulses. One purpose of this paper is to show that some important conclusions about the shape of the laser pulses may be drawn from this observation.

The theory of transient stimulated Brillouin[7] and Raman[8] scattering has been developed for the case that the input laser power is a step function. If coupling to anti-Stokes and higher-order Stokes waves may be ignored, the stimulated Raman effect is described by a set of four coupled equations[9,10] for the laser field, the population difference in the initial and final vibrational states, the Stokes field, and the normal vibrational mode of the material system, corresponding to the off-diagonal elements of the density matrix connecting the initial and final states. The interest in the present paper is focused on the transient buildup of the Stokes and vibrational oscillations. The laser field will therefore be treated as a prescribed, but time-dependent parameter, and the population difference will be taken as constant. In other words, the effects of laser-pump depletion and saturation of the material system are ignored.

In the usual manner,[11] the fields are expressed in terms of the slowly varying complex amplitudes by

$$\mathcal{E}_L = E_L(z,t)\, e^{ik_L z - i\omega_L t} \quad , \tag{1a}$$

$$\mathcal{E}_S = E_S(z,t)\, e^{ik_S z - i\omega_L t} \quad , \tag{1b}$$

$$Q_{ph} = Q(z,t)\, e^{ik_{ph} z - i\omega_{ph} t} \quad , \tag{1c}$$

where the wave vectors and frequencies are chosen to satisfy the conditions corresponding to conservation of momentum and energy, respectively,

$$k_L = k_S + k_{ph} \quad , \tag{2a}$$

$$\omega_L = \omega_S + \omega_{ph} \quad . \tag{2b}$$

The frequencies in Eq. (2b) are related to the wave vectors in Eq. (2a) by the dispersion relations of the linear medium. The parametrically coupled equations for the Stokes and vibrational complex amplitudes then assume the form[11]

$$\frac{\partial Q^*}{\partial t} + v_{ph}\frac{\partial Q^*}{\partial z} + \Gamma Q^* = i\kappa_1 E_S E_L^*(z,t) \quad , \tag{3a}$$

$$\frac{1}{v_S}\frac{\partial E_S}{\partial t} + \frac{\partial E_S}{\partial z} = -i\kappa_2 Q^* E_L(z,t) \quad . \tag{3b}$$

In these equations v_{ph} and v_S are the group velocities of the vibrational and Stokes waves, respectively; Γ^{-1} is the damping or dephasing time of the optical phonon wave. The parametric coupling constants are proportional to the change in molecular polarizability with the vibrational coordinate